

Chapter 1

UHMWPE/OPA Composite Coatings on Ti6Al4V Alloy as Protective Barriers in a Biological-Like Medium



K. Anaya-Garza, M. A. Domínguez-Crespo, A. M. Torres-Huerta, S. B. Brachetti-Sibaja, and J. Moreno-Palmerin

Abstract The formation of coatings onto the surface of Ti alloys has been used to enhance their corrosion resistance. Dip-coating is a method that can produce controllable coatings using a wide variety of molecules. Coatings based on ultra-high-molecular-weight polyethylene (UHMWPE or PE) have exhibited low friction coefficients and long wear life. It has also been reported that the formation of octadecylphosphonic acid (OPA) coatings onto the surface of various alloys prevents the corrosion process. In this work, Ti6Al4V alloy substrates were coated with UHMWPE/OPA films using the dip-coating method to evaluate their performance as protective barriers against the corrosion process in phosphate-buffered saline biological medium, to evaluate their potential application in medical implants. An analysis of the film structure and electrochemical characterizations were carried out in the as-obtained coatings. The best performance was achieved in samples immersed during 40 s (UHMWPE) followed by a most prolonged immersion in OPA (30 h). In this system, the corrosion rate was reduced up to $0.000053 \mu\text{m year}^{-1}$ with an estimated efficiency of 100%. The synergy of UHMWPE/OPA coatings displays an adequate adherence with a considerable increase in the properties against corrosion.

Keywords Ti6Al4V substrates · Biomaterials · UHMWPE/OPA films · Mechanical properties · Properties against corrosion

K. Anaya-Garza
CICATA-Altamira, Instituto Politécnico Nacional, Altamira, México

M. A. Domínguez-Crespo (✉) · A. M. Torres-Huerta (✉)
UPIIH, Instituto Politécnico Nacional, Hidalgo, México
e-mail: mdominguezc@ipn.mx

S. B. Brachetti-Sibaja
IT de Ciudad Madero, Tecnológico Nacional de México, Tamps, México

J. Moreno-Palmerin
Universidad de Guanajuato, Guanajuato, México
e-mail: jmoreno@ugto.mx

© The Author(s), under exclusive license to Springer Nature
Switzerland AG 2022

D. K. Ashish, J. de Brito (eds.), *Environmental Concerns and Remediation*,
https://doi.org/10.1007/978-3-031-05984-1_1

1.1 Introduction

Currently, medical implants with the greatest demand are those that aid in the alleviation of degenerative and inflammatory diseases that affect the bone and joints. These diseases include degenerative osteoarthritis, degenerative arthritis, rheumatoid arthritis, osteonecrosis, congenital hip conditions, neoplasia, and osteoporosis. All these conditions generate pain or loss of mechanical properties of the bone and/or joint, resulting in the removal of the orthopedic devices [1–3]. The characteristics necessary for a material to be used as a medical implant are those that possess bone-like, mechanical properties, which are neither toxic nor carcinogenic, and will not elicit an immunological response, being biocompatible, and have high corrosion resistance. Moreover, they are also known as biomaterials and can be produced from ceramic, metallic, polymer, glass, cell, or living tissue materials. Biomaterials are mainly used as plates, screws, joint replacements, orthodontic cables, femoral stems, supports for heart valves, and dental implants [4, 5].

Most of the metals used as medical implants are stainless steel, magnesium, titanium, cobalt, and their alloys. Ti6Al4V alloys can present three different phases α , β , and α' martensite; this alloy is not only used in orthopedic applications, but it has also been used in other applications such as automotive, aerospace, and chemical industries [6, 7]. Ti6Al4V has been employed as an orthopedic material mainly due to its characteristically excellent biocompatibility and adequate corrosion resistance [8, 9]. Nonetheless, it has been shown that Ti6Al4V presents considerable disadvantages such as unreliable friction coefficient and low load-carrying capacity. Thus, its mechanical integrity and superficial function are compromised, producing biological reactions and the release of vanadium, leading to the aseptic loss of the implant [10–12]. Titanium can generate reactive oxygen species by adsorption process, for example, the radical's superoxide (O_2^-) and hydroxyl (OH^-); these radicals can induce damage to biomolecules inside the host (DNA, proteins, lipids, among others). The metallic particles released by metallic biomaterials can cause osteolysis due to an immune reaction related to hypersensitivity [13–15]. Titanium particles released by orthopedic implants have been reported to invade lung, liver, and spleen triggering, an immune response, pain, and implant failure [16, 17]. Metal-on-metal joints can release between 6.7×10^{12} and 2.5×10^{14} particles per year; most of these particles displayed a particle size lower than 50 nm, but they can also achieve dimensions above 150 nm. In this context, the acceptable limits in the body for food-grade materials are from 0.4 to 5 mg/kg body weight per day of TiO_2 particles. Consequently, regarding these liabilities, there have been proposed surface modifications to metals and alloys, including coatings, thus improving their wear conditions and corrosion resistance [18, 19]. Coating treatments must meet the corresponding requirements of a biomaterial and, at the same time, increase the barrier properties avoiding a loss of the mechanical properties, present high adhesion and roughness, and avoid excessive weight in the final device, and the cost-benefit ratio must be much higher than the one presented by an implant without a surface modification process. Wetting techniques have been used due to their

simplicity and low cost, as well; through them, surface coatings can be achieved with suitable packaging, and these can be controllable using a wide variety of molecules, especially through the dip-coating method [18].

Therefore, with these disadvantages, there have been proposed surface modifications to metals and alloys, including coatings, thus improving their wear conditions and corrosion resistance [18, 19]. Coating treatments must meet the corresponding requirements of a biomaterial and, at the same time, increase the barrier properties avoiding a loss of the mechanical properties, present high adhesion and roughness, and avoid excessive weight in the final device, and the cost-benefit ratio must be much higher than the one presented by an implant without a surface modification process. Wetting techniques have been used due to their simplicity and low cost, as well; through them, surface coatings can be achieved with suitable packaging, and these can be controllable using a wide variety of molecules, especially through the dip-coating method [18].

To improve the mechanical properties of Ti6Al4V alloy, the application of polymer coatings has been used particularly in coatings of ultrahigh-molecular-weight polyethylene (UHMWPE, also referred as PE). This polymer has a carbon backbone that can fold into ordered crystalline chains (lamellae) embedded within amorphous regions. This polymer is typically employed to manufacture total joint replacements since it possesses desirable characteristics such as high abrasion and wear resistance, chemical inertness, structural strength, and biocompatibility [19–21]. Used as a coating on various alloys, UHMWPE has been reported to exhibit low friction coefficients and a long wear life [21–23]. Notwithstanding all the characteristics before mentioned, the wear properties of this polymer once it coats the surface of metallic materials present the opportunity to improve the interaction of UHMWPE/metal interphase, the resulting wear debris by friction between the two components triggers inflammatory reactions, which leads to implant failure [24–26]. Another solution to improve the corrosion resistance of metallic substrates is alkyl phosphonic acid (R-PO(OH)₂) coatings. These are formed by linear amphiphilic chains that can form M-O-P bonds with various metals such as Ti, Zr, Zn, and Al, among others [27]. The formation of octadecylphosphonic acid (OPA) films onto the surface alloys has prevented the corrosion process, increasing their wear resistance [28, 29]. It has also been reported that OPA coatings have a lubricant effect, decreasing the friction coefficient of metallic surfaces [30–32].

Metallic biomaterials are used as orthopedic implants due to their excellent mechanical properties; however, they have low wear and corrosion resistance; these drawbacks can lead to implant failure. In the present work, employing the dip-coating technique, Ti6Al4V substrates were coated with UHMWPE and OPA films. To improve the adhesion and electrochemical properties of these films in a biological-like medium (phosphate-buffered saline), the synthesis parameters were optimized [33]. Those coatings with the best corrosion resistance properties were applied to produce a composite UHMWPE/OPA coating. The UHMWPE, OPA, and UHMWPE/OPA coatings were evaluated through structural (XRD, X-ray diffraction) and electrochemical characterizations.

1.2 Materials

Disc-shaped samples of Ti6Al4V alloy (diameter of 20 mm and 2 mm of thickness) were used in this study. The titanium alloy was acquired from a local Mexican company, and the nominal composition contains V (~4.0 wt.%), Al (6.0 wt.%), Fe (0.04 wt.%), C (0.08 wt.%), N (0.05 wt.%), O (0.2 wt.%), H (0.014 wt.%), and Ti (balance).

UHMWPE powder with a particle size of 125 μm (M_w 3×10^6 – 6×10^6 mol.wt.), octadecylphosphonic acid (97%), decahydronaphthalene (99% purity), and phosphate-buffered saline solution were purchased from SIGMA-Aldrich Inc; ethanol (96%) from FERMONT.

1.3 Experimental Methods

1.3.1 Surface Preparation

The process of surface preparation of the substrates begins by polishing them using grit SiC emery paper grade from 400 to 1500; then, they were washed in an ultrasonic bath with distilled water, ethanol, and acetone solutions; finally, the samples were dried at room temperature.

1.3.2 Synthesis of UHMWPE Coatings

The Ti6Al4V substrates were coated with UHMWPE films using a UHMWPE solution prepared with 2.3 g of UHMWPE powder dissolved in 50 mL of decalin (5 wt.%) inside a three-necked flask. Subsequently, the three-necked flask was placed connected to a reflux condenser and placed into a sand bath. The solution was heated until the solution reached 80 °C (20 min), followed by heating up to 185 °C (2 h). The coated samples were obtained using various immersion times (20, 30, and 40 s); immediately thereupon, these samples were dried at 100 °C (20 h). Finally, the samples were cooled down at room temperature.

1.3.3 Synthesis of Octadecylphosphonic Acid Coatings/ UHMWPE-OPA Coatings

The formation of the OPA films deposited onto the Ti6Al4V alloys and UHMWPE-coated Ti6Al4V alloys were realized using a solution of octadecylphosphonic acid which was prepared with 0.1724 g of octadecylphosphonic acid powder dissolved

in 50 mL of ethanol to reach a balance of 1 mM inside a three-necked flask. Afterward, the three-necked flask was connected to a reflux condenser and placed into a sand bath, and the solution was heated up to 40 °C (2 h). Subsequently, this solution was placed in a beaker of the model Dip Coating WHL-30B immersion equipment. The coated samples were settled on a controlled speed arm. To acquire the OPA-coated samples, various immersion times were used (20 and 30 h); then those samples were dried at 80 °C (4 h) and then cooled down at room temperature. The UHMWPE-OPA coatings were realized using 40 s and 30 h of immersion time in UHMWPE solution and octadecylphosphonic acid solution, respectively.

1.3.4 Structural Characterization

The structural characterization of the UHMWPE, OPA, and UHMWPE/OPA samples was evaluated through X-ray diffraction (XRD), using a Bruker D8 advanced diffractometer (LYNXEYE detector). The XRD patterns of all the samples were collected using CuK radiation ($\lambda = 0.15406$ nm) within a range of 5–90° (2 θ) at a scan rate of 2°min⁻¹. Employing an elcometer tester (Elcometer E456), the dry thickness of these coatings was evaluated.

1.3.5 Electrochemical Characterization

Electrochemical measurements were realized in a typical three-electrode cell using a Gamry reference (600 series) potentiostat/galvanostat. The analyses were carried out using a work electrode area of 0.7 cm². Saturated calomel electrode (SCE) was used as reference electrode and a graphite bar as counter electrode. All the samples were stabilized for 30 min in the PBS electrolyte before the evaluations. All measurements were conducted by triplicate. Tafel plots were evaluated using a potential range of ± 250 mV_{OCP} by applying 1 mV s⁻¹ of scan rate at room temperature. Gamry Instruments DC105™ DC corrosion technique software was used to determine the kinetic parameters of the as-prepared samples. The corrosion rate was computed from Faraday's law using the following equation:

$$CR = (i_{\text{corr}} K EW) / d \quad (1.1)$$

In the formula, the corrosion rate is represented by CR ($\mu\text{m year}^{-1}$), d represents the density (g cm^{-3}), EW represents the equivalent weight, $3.272 \times 10^6 \mu\text{m A}^{-1} \text{cm}^{-1} \text{year}^{-1}$ is the constant in the equation (K), and i_{corr} is the corrosion current density (A cm^{-2}).

The protection efficiency percentage estimation was also calculated using the classical relation between the corrosion current densities of the uncoated ($i_{\text{corr},0}$) and coated samples ($i_{\text{corr},i}$), with UHMWPE, OPA, and UHMWPE/OPA:

$$PEF\% = \left(\frac{[i_{\text{corr}}, 0 - i_{\text{corr}}, i]}{i_{\text{corr}}, i} \right) \times 100\% \quad (1.2)$$

Similarly, the estimation of the porosity of each system (UHMWPE, OPA, and UHMWPE/OPA) was calculated using the following equation:

$$P = \left(R_{\text{pbs}} / R_{\text{pc}} \right)_{\times} 10 \left(-\Delta E_{\text{corr}} / \beta_a \right) \times 100\% \quad (1.3)$$

where P is porosity and R_{pbs} and R_{pc} are the polarization resistances of the bare substrate and the resistance of the UHMWPE-, OPA-, and UHMWPE-/OPA-coated samples, respectively. ΔE_{corr} is the difference of the corrosion potentials between the bare substrate and the coated samples, and β_a characterizes the anodic Tafel slope of the Ti6Al4V.

Finally, the barrier properties were analyzed by electrochemical impedance spectroscopy (EIS) measurements. The spectra were acquired within the frequency range 100 kHz–10 mHz (with 10 mV of a sinusoidal voltage signal applied). The experimental data of each spectra were fitted through equivalent circuits using the Zview2 version 3.3 program. The equivalent circuit models of the plots reported were considered acceptable when the χ^2 values were lower than 10^{-2} .

1.4 Results and Discussion

1.4.1 Structural Characterization

The XRD patterns of UHMWPE and OPA powders, as well as bare and coated Ti6Al4V substrates (OPA, UHMWPE and UHMWPE/OPA) are shown in Fig. 1.1. Based on the XRD patterns, the as-prepared UHMWPE and UHMWPE/OPA coatings show classical peaks of polyurethane located at 21.32° (110) and 23.5° (200) in the θ – 2θ region, PDF # 53-28-59 chart.

Although the OPA XRD pattern has not been found indexed in literature, the rise of new peaks in the OPA and UHMWPE/OPA XRD patterns between ~ 10 and 20° (θ – 2θ) are representatives of the presence of OPA on the surface of the bare and UHMWPE-coated Ti6Al4V alloy [33–35]. According to the PDF #44-1294 file, all XRD patterns showed the orientation of the Ti6Al4V in the cubic β -Ti phases and hexagonal α -Ti, between ~ 35 – 41° and 77° (θ – 2θ) [36].

1.4.2 Electrochemical Measurements

In the Tafel plots shown in Fig. 1.2, displacements in the corrosion potential to more positive values are observed in the polarization curves for all the coated samples. OPA-coated samples exhibit a corrosion potential of $-0.022 V_{\text{SCE}}$; it heightened up

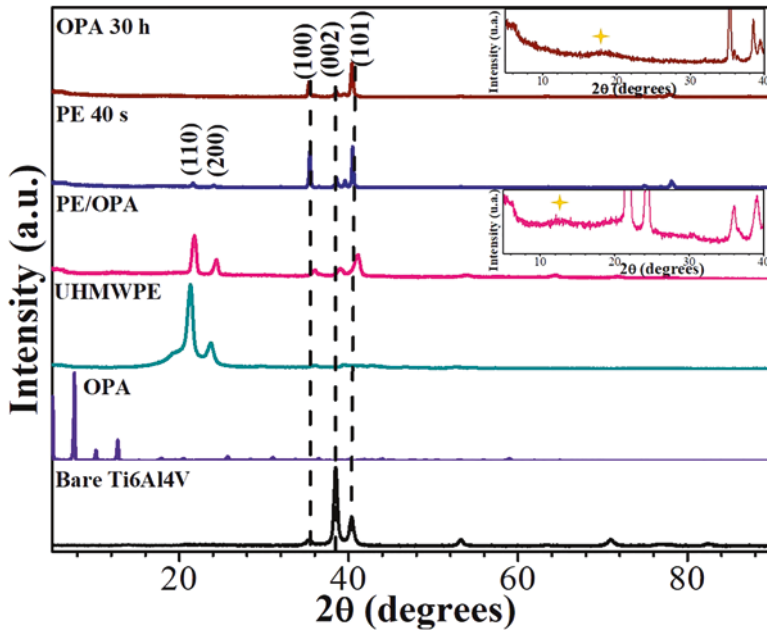


Fig. 1.1 XRD patterns of UHMWPE and OPA powders and bare and coated samples

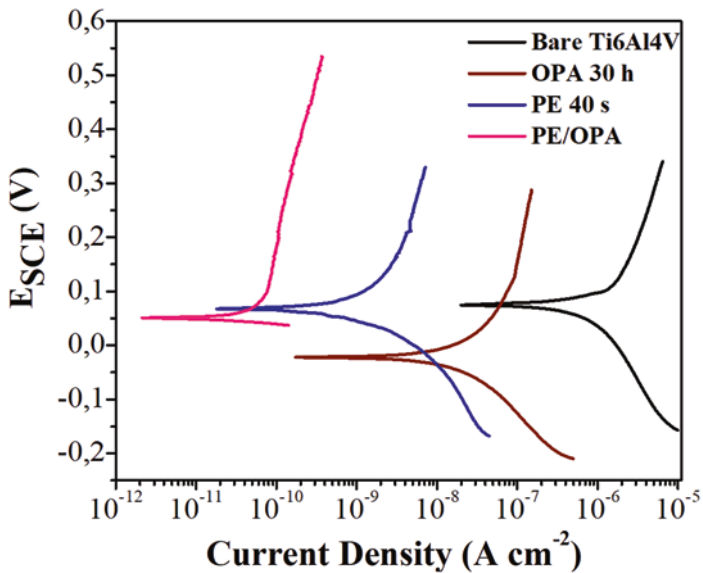


Fig. 1.2 Tafel polarization curves of bare substrate and (UHMWPE, OPA, and UHMWPE/OPA) coated samples in PBS

to similar values as the bare samples ($0.074 V_{SCE}$), 0.067 , and $0.051 V_{SCE}$ for PE 40 s and UHMWPE/OPA, respectively. Based on the mixed potential theory, due to the attack of the electrolyte (phosphate-buffered saline solution) charged particles in the anodic region, a change in the number of the corrosion potential can be seen [33]. The plot shows a clear displacement toward lower corrosion current density values after coating the Ti6Al4V alloys, particularly with the UHMWPE/OPA coatings. The diminishing of the corrosion rate is correlated with the reduction of the charge transfer resistance between the coated metal and the electrolyte. Then, the decrease of the corrosion current density values seen in the polarization curves of the coated samples indicates a lower charge transfer resistance and, accordingly, a slower corrosion rate.

The cathodic Tafel slopes were calculated employing the polarization curves; a reduction from $-458 \text{ mV decade}^{-1}$ reaching values between 45 and $292 \text{ mV decade}^{-1}$ for the UHMWPE, OPA, and UHMWPE/OPA coatings (Table 1.1) can be observed. Contrary, the anodic Tafel slopes were not calculated since they tend to form a pseudo passive region. The UHMWPE/OPA coatings presented the lowest corrosion densities ($3 \text{ E-6 } \mu\text{A cm}^{-2}$), almost six orders in magnitude lower than the bare alloy ($2.371 \mu\text{A cm}^{-2}$). While UHMWPE and OPA coatings acted as good barriers against the corrosion process on their own, once the UHMWPE/OPA coating was formed, the barrier properties were enhanced, and the corrosion rate exhibited a considerable deceleration from 41.26 to $5.3 \text{ E-5 } \mu\text{m year}^{-1}$.

The estimation of the protection efficiency ($P_{EF} \%$) of the UHMWPE, OPA, and UHMWPE/OPA coatings was calculated, from the polarization curves and Eq. (1.2) (using the corrosion current density values). The coatings present efficiencies from 97 for OPA coatings up to $\sim 100\%$ for the UHMWPE/OPA coatings, whereas UHMWPE coatings achieved 99.9% . From Eq. (1.3), the porosity of the coatings was estimated; the UHMWPE/OPA composite coatings presented a noteworthy diminishing of the porosity compared to the individual coatings; this indicates a uniform coating with fewer defects (Table 1.1).

Figure 1.3 shows EIS plots of the bare and coated Ti6Al4V alloys immersed in a PBS solution. The Nyquist plot (Fig. 1.3a) shows that the semicircle of the impedance of the bare specimens was around $24 \text{ k}\Omega \text{ cm}^{-2}$ and increased up to $\sim 1.8 \text{ M}\Omega \text{ cm}^{-2}$, $24.8 \text{ M}\Omega \text{ cm}^{-2}$, and $400 \text{ M}\Omega \text{ cm}^{-2}$ when coated with OPA, UHMWPE, and UHMWPE/OPA films, respectively. The size of the radius of the semicircle in the Nyquist plots is associated with the charge transfer resistance; the increase of the

Table 1.1 Kinetic parameters of the bare substrate and (UHMWPE, OPA, and UHMWPE/OPA) coated samples in PBS

Sample	E_{corr} (VSCE)	I_{corr} ($\mu\text{A cm}^{-2}$)	β_c (mV/ dec)	% Porosity	$P_{EF}\%$	CR ($\mu\text{m year}^{-1}$)
Bare Ti6Al4V	0.074	2.371	-458	-	-	41.28
OPA 30 h	-0.022	6.8E-2	-292	7.11	97	1.19
PE 40 s	0.067	3E-3	-279	0.17	99.9	0.05
PE/OPA	0.051	3E-6	-45	2E-3	100	5.3E-5

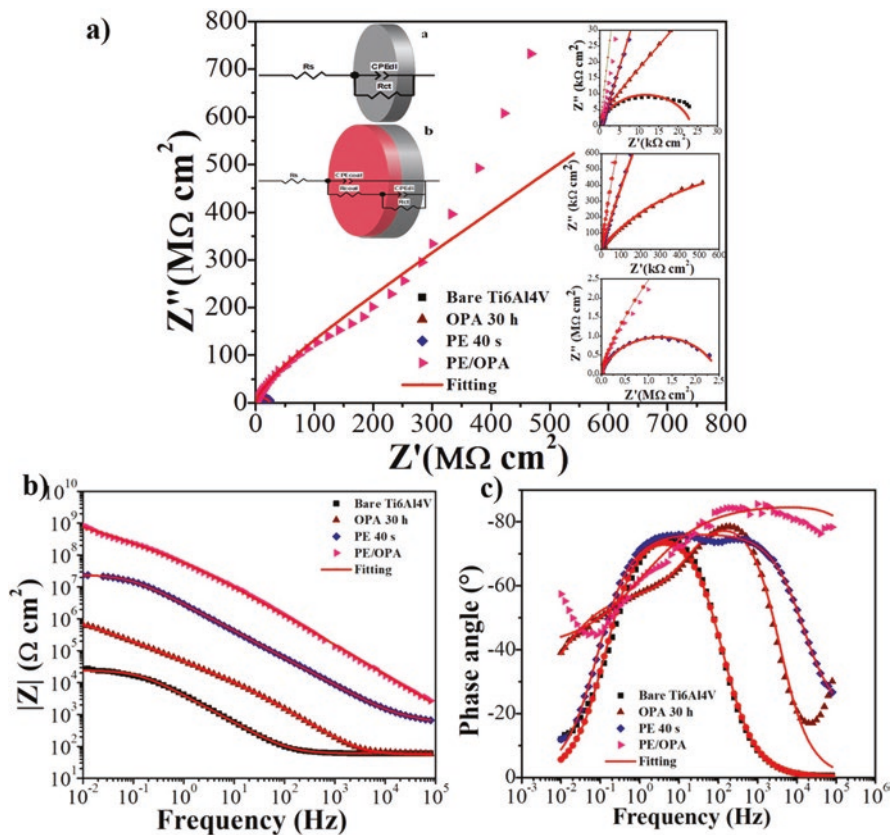


Fig. 1.3 (a) Nyquist and (b–c) Bode plots of bare substrate and (UHMWPE, OPA, and UHMWPE/OPA) coated samples in PBS

charge transfer resistance observed is related to the coatings formed onto the surface of the Ti6Al4V alloys. Figure 1.3b,c (Bode plots) show two-time constants for all the coated samples, one attributed to each coating and the other related to the charge transfer resistances.

Table 1.2 shows the values obtained from the simulation of the experimental data; two equivalent circuits were proposed. The model proposed was comprised of the resistance solution (R_s); the coating contribution was modeled, with a coating resistance (R_{coat}) in series with a coating capacitance simulated with a constant phase element (CPE_{coat}). The metal contribution consisted of the charge transfer resistance (R_{ct}) and its constant phase element (CPE_{di}) that simulates the double-layer capacitance. The sum of the resistances of the model (R_s , R_{coat} , and R_{ct}) reflects the polarization resistance (R_p) of the equivalent circuit proposed. A suitable fitting of the model was accepted when the χ^2 values were lower than 10^{-2} .

The fitting of these parameters confirms that the OPA, UHMWPE, and UHMWPE/OPA coatings diminished the charge transfer resistance, which can be

Table 1.2 Values obtained from the modeled circuit of the bare substrate and (UHMWPE, OPA, and UHMWPE/OPA) coated samples in PBS

Sample	CPE _{coat}			CPE _{dl}			χ^2 (10 ⁻³)	Equiv. circuit	
	R_s	Y_{O1coat}	R_{coat}	Y_{O2dl}	R_{ct}				
	(Ω cm ²)	(Ω^{-1} cm ² sn)	n1 (Ω cm ²)	(Ω^{-1} cm ² sn)	n2 (Ω cm ²)				
Bare Ti6Al4V	59.24	–	–	–	4.73E-5	0.87	24.43E3	2.49	a
OPA 30 h	55.93	1.66E-8	0.92	17.19E3	5.44E-6	0.59	1.84E6	13.41	b
UHMWPE 40s	412.1	2.91E-8	0.85	741	4.04E-8	0.85	2.48E7	0.62	b
UHMWPE/OPA	137.5	11.5E-9	0.94	1.12E3	4.33E-12	0.45	811.5E9	6.37	b

seen by a deceleration of the corrosion rate of the Ti6Al4V alloys, especially when coated with the UHMWPE/OPA film.

1.5 Conclusions

In this study, the dip-coating technique to optimize the process of coating Ti6Al4V substrates with OPA and UHMWPE films in order to improve its corrosion resistance properties in a biological-like medium (phosphate-buffered saline) was used. From the above results, the following conclusions were obtained: whereas all the coatings delayed the interaction between the alloy surface and the ions in the electrolyte, the performance of the barrier properties of the composite coating as a result of combined adding of the OPA coating over the UHMWPE coating is enhanced, which can be potentially favorable for biomedical applications. An estimated efficiency of $\sim 100\%$ accompanied by a reduction in the porosity percentage values was observed for the coated Ti6Al4V/UHMWPE/OPA systems. The barrier properties that showed these samples reduced the corrosion rate up to $5.3 \text{ E-}5 \mu\text{m year}^{-1}$, which was much better than the electrochemical performance of individual systems (Ti6Al4V/OPA or Ti6Al4V/UHMWPE). An important drawback to consider is the long immersion time that is required for OPA deposition, but it is believed that cost-benefit is still adequate for biomedical applications. In order to confirm this assumption, the evaluations of biocompatibility and bioactivity as well as in vitro and in vivo studies are in progress.

Acknowledgments K. Anaya-Garza is obliged to her postgraduate fellowship to CONACYT (492198) and SIPIPN. The authors are also grateful for the financial support provided by the Instituto Politécnico Nacional through the SIP2022-0668, SIP2022-0671, SIP2022-1153, and 2022-1155 projects, CONACYT CB2015-252181 project, and SNI-CONACYT.

References

1. Y. Liu, Role of implants surface modification in osseointegration: A systematic review. *J. Biomed. Mater. Res. A* **108**(3), 470–484 (2020)
2. H.M. Kremers, Clinical factors, disease parameters, and molecular therapies affecting osseointegration of orthopedic implants. *Curr. Mol. Biol. Rep.* **2**(3), 123–132 (2016)
3. M. Geetha, Ti based biomaterials, the ultimate choice for orthopaedic implants—A review. *Prog. Mater. Sci.* **54**(3), 397–425 (2009)
4. N.M. Everitt, Characterisation of fretting-induced wear debris for Ti-6Al-4 V. *Wear* **267**(1-4), 283–291 (2009)
5. R.S. Magaziner, Investigation into wear of Ti-6Al-4V under reciprocating sliding conditions. *Wear* **267**(1-4), 368–373 (2009)
6. R. Singh, Corrosion degradation and prevention by surface modification of biometallic materials. *J. Mater. Sci. Mater. Med.* **18**(5), 725–751 (2007)
7. C. Veiga, Properties and applications of titanium alloys: A brief review. *Rev. Adv. Mater. Sci* **32**(2), 133–148 (2012)
8. E. Almanza, Corrosion resistance of Ti-6Al-4V and ASTM F75 alloys processed by electron beam melting. *J. Mater. Res. Technol.* **6**(3), 251–257 (2017)
9. J. Grabarczyk, Tribocorrosion behavior of Ti6Al4V alloy after thermo-chemical treatment and DLC deposition for biomedical applications. *Tribol. Int.* **153**, 106560 (2021)
10. B.C. Costa, Vanadium ionic species from degradation of Ti-6Al-4V metallic implants: In vitro cytotoxicity and speciation evaluation. *Mater. Sci. Eng. C* **96**, 730–739 (2019)
11. M. Dalmiglio, The effect of surface treatments on the fretting behavior of Ti-6Al-4V alloy. *J. Biomed. Mater. Res. B. Appl. Biomater. Off. J. Soc. Biomater. Jpn. Soc. Biomater. Aust. Soc. Biomater. Korean Soc. Biomater.* **86**(2), 407–416 (2008)
12. F. Javed, Is titanium sensitivity associated with allergic reactions in patients with dental implants? A systematic review. *Clin. Implant Dent. Relat. Res.* **15**(1), 47–52 (2013)
13. P. Doorn, Metal wear particle characterization from metal on metal total hip replacements: Transmission electron microscopy study of periprosthetic tissues and isolated particles. *J. Biomed. Mater. Res. Off. J. Soc. Biomater. Jpn. Soc. Biomater. Aust. Soc. Biomater.* **42**(1), 103–111 (1998)
14. B.D. Ratner, Healing with medical implants: The body battles back. *Sci. Transl. Med.* **7**(272), 272fs4-272fs4 (2015)
15. S.M.P. Rossi, Ten-year outcomes of a nitrided Ti-6Al-4V titanium alloy fixed-bearing total knee replacement with a highly crosslinked polyethylene-bearing in patients with metal allergy. *Knee* **27**(5), 1519–1524 (2020)
16. D. Olmedo, An experimental study of the dissemination of titanium and zirconium in the body. *J. Mater. Sci. Mater. Med.* **13**(8), 793–796 (2002)
17. F. Yildiz, Plasma nitriding behavior of Ti6Al4V orthopedic alloy. *Surf. Coat. Technol.* **202**(11), 2471–2476 (2008)
18. X. Tang, Dip-coating for fibrous materials: Mechanism, methods, and applications. *J. Sol-Gel. Sci. Technol.* **81**(2), 378–404 (2017)
19. T. Chang, Tribological behavior of aged UHMWPE under water-lubricated condition. *Tribol. Int.* **133**, 1–11 (2019)
20. Y. Wang, Friction, and wear characteristics of ultrahigh molecular weight polyethylene (UHMWPE) composites containing glass fibers and carbon fibers under dry and water-lubricated conditions. *Wear* **380**, 42–51 (2017)
21. S.M. Kurtz, *The UHMWPE Handbook: Ultra-High Molecular Weight Polyethylene in Total Joint Replacement* (Ed. Elsevier, San Diego, 2004)
22. F.W. Shen, in M. Jenkins., *Biomedical Polymers* (Ed. Woodhead Publishing, Boca Raton, 2007)
23. M. Hussain, Ultra-high-molecular-weight-polyethylene (UHMWPE) as a promising polymer material for biomedical applications: A concise review. *Polymers* **12**(2), 323 (2020)

24. M. Samad, Tribology of UHMWPE film on air-plasma treated tool steel and the effect of PFPE overcoat. *Surf. Coat. Technol.* **204**(9-10), 1330–1338 (2010)
25. A. Chih, Frictional and mechanical behaviour of graphene/UHMWPE composite coatings. *Tribol. Int.* **116**, 295–302 (2017)
26. B. Panjwani, Tribological characterization of a biocompatible thin film of UHMWPE on Ti6Al4V and the effects of PFPE as top lubricating layer. *J. Mech. Behav. Biomed. Mater.* **4**(7), 953–960 (2011)
27. G. Guerrero, Anchoring of phosphonate and phosphinate coupling molecules on titania particles. *Chem. Mater.* **13**(11), 4367–4373 (2001)
28. M. Kosian, Structure and long-term stability of alkylphosphonic acid monolayers on SS316L stainless steel. *Langmuir* **32**(4), 1047–1057 (2016)
29. E. Mioč, Modification of cupronickel alloy surface with octadecylphosphonic acid self-assembled films for improved corrosion resistance. *Corros. Sci.* **134**, 189–198 (2018)
30. J.P. Soullier, Octadecylphosphonic acid self-assembled monolayers as lubricant coatings stable in alkaline media, in *Symposium EE – Organic/Inorganic Hybrid Materials on MRS Online Proceedings Library (OPL)*, (Cambridge University Press, Boston, 2004), pp. 299–304
31. S. Prunte, Molecular coverage determines sliding wear behavior of n-octadecylphosphonic acid functionalized Cu–O coated steel disks against aluminum. *Materials* **13**(2), 280 (2020)
32. D. Hill, Study of the tribological properties and ageing of alkylphosphonic acid films on galvanized steel. *Tribol. Int.* **119**, 337–344 (2018)
33. K. Anaya-Garza, Electrochemical performance of UHMWPE biocompatible coatings on Ti6Al4V alloy in simulated body solutions: Influence of immersion time. *ECS Trans.* **101**(1), 325 (2021)
34. B.H. Bac, Surface-modified aluminogermanate nanotube by OPA: Synthesis and characterization. *Inorg. Chem. Commun.* **12**(10), 1045–1048 (2009)
35. Y. Sun, A molecular-level superhydrophobic external surface to improve the stability of metal–organic frameworks. *J. Mater. Chem. A* **5**(35), 18770–18776 (2017)
36. C. Cai, In-situ integrated fabrication of Ti–Ni coating during hot isostatic pressing of Ti6Al4V parts: Microstructure and tribological behavior. *Surf. Coat. Technol.* **280**, 194–200 (2015)